Influence of Annealing Temperature on Berthelot-Type Hopping Conduction Mechanism in Carbon-Nickel Composite Films

V. Dalouji[1**], S. M. Elahi[2], A. Ghaderi[3], S. Solaymani[3]

[1]*Department of Physics, Malayer University, Malayer, Iran*
[2]*Plasma Physics Research Center, Science and Research Branch, Islamic Azad University, Tehran, Iran*
[3]*Young Researchers and Elite Club, Kermanshah Branch, Islamic Azad University, Kermanshah, Iran*

(Received 15 December 2015)

Electrical conductivity of carbon-nickel composite films annealed at temperatures 300, 500 and 800°C is studied over a temperature range of 50–300 K. While the conductivity data above room temperature show extended state conduction, lowering the temperature from 150 to 50 K leads to the Berthelot-type conduction mechanism. It can be seen that the films annealed at 500°C have the maximum conductivity. The extent of the carrier wave function at 500°C has the minima 2.87×10^{-7} *cm and* 2.45×10^{-7} *cm in octahedral-metal stretching vibrations and intrinsic stretching vibrations of the metal at the tetrahedral site, respectively. The average distances between two vibration octahedral and tetrahedral sites at 500°C also have the minima* 1.13×10^{-7} *cm and* 0.97×10^{-7} *cm, respectively. The Berthelot temperature for films annealed at 800°C has the minimum of 94.3 K.*

PACS: 72.15.Eb, 66.70.Df DOI: 10.1088/0256-307X/33/5/057203

Thin-film materials have many interesting properties in optic, electronic, coating technology and surface morphology.[1–4] The electrical and optical properties of matrixes can be affected by metal doping.[5,6] The advantage of amorphous carbon matrix-metal (a-c: Me) films as electronic materials is due to their conductivity behavior, which can be changed from dielectric to metallic by slight variation in their composition.[7] Our special deposition conditions including room temperature and nonwet chemical deposition are appropriate for applications in optical and electronic devices.[8] There are a few reports on the study of electrical properties of carbon–nickel composite films. However, less attention has been paid to the conduction mechanism of carbon–nickel composite films. In the previous reports, we have studied the effect of deposition time and annealing temperature on magnetic and optical properties of the C–Ni films.[9–12] In the present work, we investigate the effect of annealing temperature on the conduction mechanism of C–Ni composite films in low temperature 50–150 K.

The films were grown at room temperature by rf-magnetron sputtering on quartz substrates using a mosaic target in a deposition chamber evacuated to a base pressure of 5×10^{-5} mbar, and then the constant Ar working pressure of 4×10^{-2} mbar was settled and maintained by a throttle valve. Deposition was carried out in constant rf power regime 400 W. The angle of incident ions with target surface was 90°, and the substrate–target distance was 60 mm. The films were prepared at the same deposition time of 600 s and then heat treated at 300, 500 and 800°C under ambient atmospheric pressure in a furnace for 2 h. The field emission scanning electronic microscopy (FESEM) images were used for the morphological characterization. The Rutherford backscattering (RBS) spectra were obtained by using incident ions (^{4}He) with energy of 2 keV for Ni concentration measurement. The direct current electrical conductivity was measured by cooling samples in a continuous He flow in cryogenic units (the optical low temperature model CCS 450 USA) in a thermostatic chamber in the temperature range of 50–300 K. ORTEC (456, USA, 0–3 kV) high-voltage power supply, Metrix VX102A (FRANCE) and Keithley 196 system DMM (USA) electrometers in the temperature range 50–300 K, were used for voltage and current measurements, accordingly.

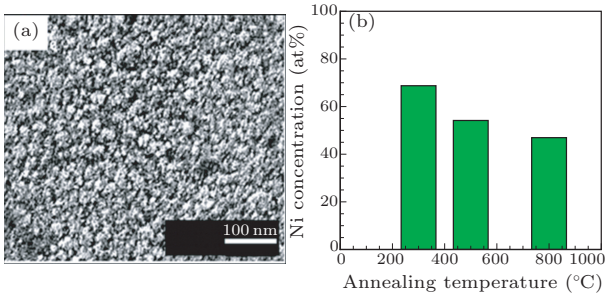

Fig. 1. The FESEM image of C–Ni films annealed at 800°C (a) and the Ni concentration in the C–Ni films annealed at temperatures 300°C, 500°C and 800°C (b).

Figures 1(a) and 1(b) show the typical FESEM image of films annealed at 800°C and the values of Ni concentration of C–Ni films annealed at different temperatures 300, 500 and 800°C, respectively. As shown in the FESEM images, the size of the nickel nanoparticles at 800°C has the value about 15 nm. The Ni content computed from the SIMN-RA software simulation of films (for layer with a thickness of 5000×10^{15} atom·cm^{-2}), showing that films contain 68.75 at%, 54.16 at% and 46.95 at% Ni at 300, 500 and

**Corresponding author. Email: dalouji@yahoo.com
© 2016 Chinese Physical Society and IOP Publishing Ltd

800℃, respectively.

Figures 2(a), 2(b) and 2(c) show the current measured for films annealed at temperatures 300, 500 and 800℃, respectively, with the reciprocal of temperature from 50 to 300 K. A single current conduction mechanism, $I = I_0 \exp(-E_a/kt)$, where k is the Boltzmann constant, and E_a is the activation energy for conduction, can be fitted to all the data.[13]

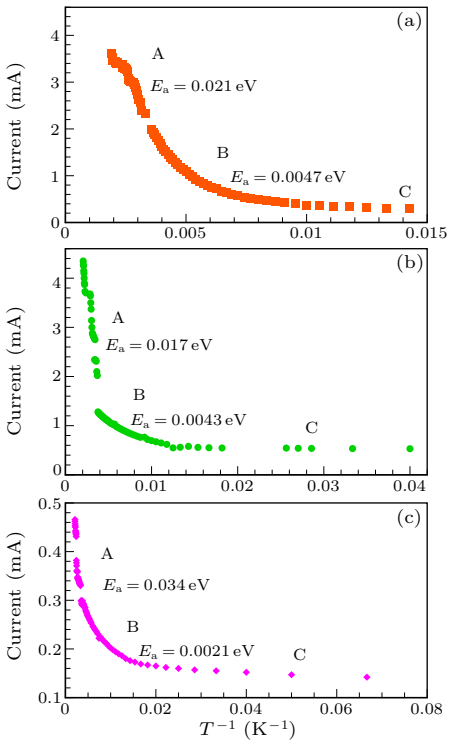

Fig. 2. The current against reciprocal temperature from 50 to 300 K for films annealed at (a) 300℃, (b) 500℃, and (c) 800℃.

Region A shows relatively fast varying current with temperature $T > 150$ K. The values of E_a for the films annealed at 300, 500 and 800℃ in this region are 0.021, 0.017, and 0.034 eV, respectively. Region B is dependent weakly on temperature and results in very small values with temperature $50 < T < 150$ K. The values of E_a for the films annealed at 300, 500 and 800℃ in this region are 0.0047, 0.0043, and 0.0021 eV, respectively. In region C, $T < 50$ K, the current becomes almost independent of T and may be explained with the variable range hopping (VRH) conduction mechanism. The values of E_a at low temperature are very low compared with the values obtained from high temperature I–T data.

Figure 3(a) shows a numerical evaluation of the differential activation energies by using the relation $E_a = -k_B \Delta \ln[\sigma(T)]/\Delta(1/T)$ for successive points of E_a for the films annealed at 300, 500 and 800℃, where $\sigma(T)$ is the conductivity in the range of 50–150 K. A fluctuation of the activation energies depending on the annealing temperature in the films is observed.[14] Therefore, a single activated term in the Arrhenius plot is inappropriate for the films in the range of 50–150 K.

In disordered systems, the carrier conduction at low temperatures may be assisted by variable range hopping given as $ln(I) \propto n(T_k/T)$, where T_k is a constant, and the value of n gives information of the type of carrier conduction mechanism and depends on the grain sizes and the temperature region.[13] For $n = -1$, it is expected that the conduction can be in the state with the Berthelot-type conduction mechanism, and T_k is a constant for the material, of which the Berthelot-type conduction k can be replaced with B. To distinguish the Berthelot type of conductions and also to obtain an insight into the possible transport mechanism from 50 to 150 K we have plotted $\ln[d \ln I/d \ln T]$ with $\ln T$ in Fig. 3(b).[15,16] The values of $n = -0.8$, -0.75 and -1.06 for the films annealed at 300, 500 and 800℃ suggest the existence of the Berthelot-type conduction within the gap near the Fermi energy.

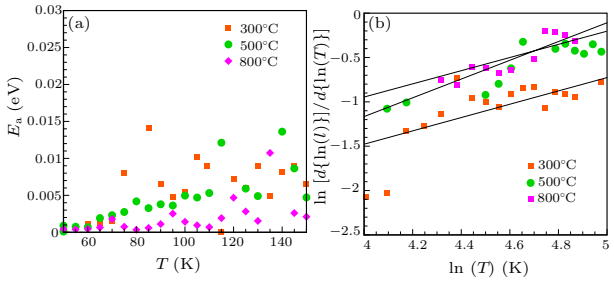

Fig. 3. (a) E_a versus temperature, and (b) $\ln[d \ln I/d \ln T]$ of the C–Ni films annealed at 300, 500 and 800℃ versus $\ln T$.

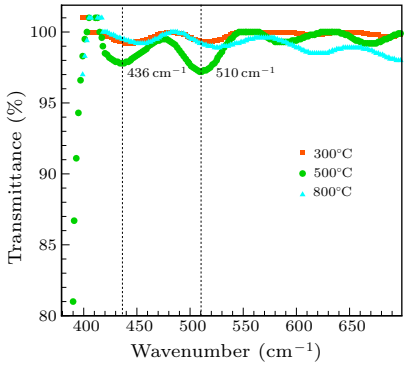

Fig. 4. The FTIR spectra of the C–Ni films annealed at 300, 500 and 800℃.

Figure 4 shows the FTIR spectra for the films annealed at 300, 500 and 800℃ in the range of wave numbers from 300 to 700 cm^{-1}. The two absorption bands observed at about 510 cm^{-1} and 436 cm^{-1} correspond to vibrations of tetrahedral and octahedral complexes, respectively. The highest one typically observed in the range of 500–600 cm^{-1} corresponds to intrinsic stretching vibrations of the metal at the tetrahedral site, $M_{tetra} \leftrightarrow O$, whereas the lowest band, typically observed in the range of 450–385 cm^{-1}, is assigned to octahedral-metal stretching vibrations, $M_{octa} \leftrightarrow O$.[17,18]

In the small polaron model of a self-trapped charged particle transferring with phonon assistance from site to site can be seen as the coincidence of the initial and final states, and secondly the tunneling during the coincidence. The transfer rate between sites has the form $R = \Gamma[v\exp(-U/k_{\rm B}T)]$, where Γ, v and U are the tunnelling probability during coincidence, a characteristic atomic vibration frequency, and activation energy for a site's displacement, respectively. If the temperature is high enough so that classical statistics can be applied, then $\Gamma = c\exp(-2\alpha S_{\rm o})\exp(2\alpha^2 k_{\rm B}T/m\omega^2)$, where c is a constant, $S_{\rm o}$ is the average distance between sites, α is the inverse of localization length, and ω is the site's variation frequency. Therefore the full expression for the transfer rate in the vibrating barrier model is given by[19–21]

$$R = c\exp(-2\alpha S_{\rm o})\exp(-U/k_{\rm B}T)\exp(2\alpha^2 k_{\rm B}T/m\omega^2).$$

Three exponential terms thus control R, the overlap term $\exp(-2\alpha S_{\rm o})$, the coincidence term $\exp(-U/k_{\rm B}T)$, and the tunneling term $\exp(2\alpha^2 k_{\rm B}T/m\omega^2)$. In the Tredgold model, the tunneling term is the dominant effect and independent of temperature, therefore the dependence of the transfer rate for the above tunneling term given by $d\log R/dT = 2\alpha^2 k_{\rm B}T/m\omega^2$. For the opposite extreme where the thermal expansion is included while the effect of the sites variation in amplitude is not, the dependence of the transfer rate for the above tunneling term is given by $d\log R/dT = -2\alpha P S_{\rm o}$, where p is the linear thermal expansion constant. Figures 5(a) and 5(b) show the variation of I and $\ln I$ with temperature for the C–Ni films annealed at 300, 500 and 800℃ in the temperature range 50–150 K. Using Fig. 5(b), the values of the Berthelot-type temperature $T_{\rm B}$ are obtained. With considering the increasing tunneling, due to the fact that the larger amplitude is 10^3 greater than the corresponding reduction due to the increased equilibrium separation of the sites and obtained values $T_{\rm B}$, the values of average distance $S_{\rm o}$ and the extents of the carrier wave function can be calculated as listed in Table 1. It is obvious that the increasing Ni concentrations cause a decrease in the distance between the Ni ions. It can be seen that with the increasing annealing temperature from 300 to 500℃, $S_{\rm o}$ decreases from 1.34×10^{-7} to 1.13×10^{-7} cm and then from 500 to 800℃ it increases to 1.52×10^{-7} for absorption bands 436 $\rm cm^{-1}$, which is in agreement with the increasing conductivity due to electron hopping from N ions. The value of $S_{\rm o}$ decreases from 1.15×10^{-7} to 0.97×10^{-7} cm for films annealed from 300 to 500℃, and from 500 to 800℃ it increases to 1.3×10^{-7} for the absorption band 510 $\rm cm^{-1}$. It can be seen that with the increasing annealing temperature up to 500℃ due to decreasing thickness hence increasing densification, the space between ions decreases. To observe the Berthelot-type conduction experimentally, the inverse localization parameter α and the average distance between the sites should be small. The extents of the carrier wave function from 300 to 500℃ decrease from 3.24×10^{-7} to 2.87×10^{-7} cm and then increase to 3.85×10^{-7} cm from 500 to 800℃ for the absorption band 436 $\rm cm^{-1}$. The extents of the carrier wave function from 300 to 500℃ decrease from 2.77×10^{-7} to 2.45×10^{-7} cm and then increase to 3.29×10^{-7} cm from 500 to 800℃ for the absorption band 510 $\rm cm^{-1}$. Therefore, it can be seen that the extents of the carrier wave function due to vibrations of Ni ions in tetrahedral at 500℃ are lower than the sites of octahedral complexes. Therefore as listed in Table 1, the type of vibration obtained from the FTIR spectra and annealing temperature can affect the hopping parameters. On the other hand, nanoparticle size and Ni concentration can be strongly affected by annealing temperature. It can be seen that the Berthelot-type conduction in vibrations of the metal at the tetrahedral site for films annealed at 500℃ is better.

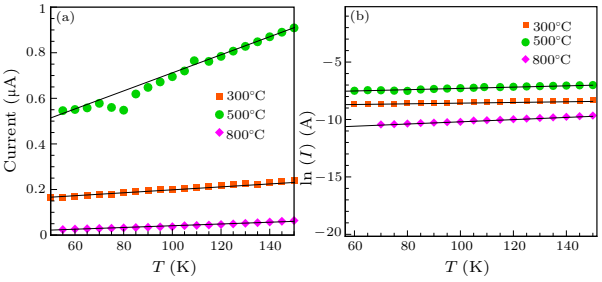

Fig. 5. (a) Dependence of current with temperature and (b) variation of $\ln I$ with temperature for C–Ni films annealed at 300, 500 and 800℃ in the temperature range 50–150 K.

Table 1. Electrical parameters of the Berthelot-type mechanism of the C–Ni films annealed at 300, 500 and 800℃.

Annealing temperature	$T_{\rm B}$ (K)	ω_1 (10^{13} $\rm s^{-1}$)	α_1^{-1} (10^{-7} cm)	S_{01} (10^{-7} cm)	ω_2 (10^{13} $\rm s^{-1}$)	α_2^{-1} (10^{-7} cm)	S_{02} (10^{-7} cm)
300℃	120	8.21	3.24	1.34	9.6	2.77	1.15
500℃	170	8.21	2.87	1.13	9.6	2.45	0.97
800℃	94.3	8.21	3.85	1.52	9.6	3.29	1.3

In conclusion, the annealing temperature plays an important role in electrical properties of the C–Ni composite films annealed in the temperature range 300–800℃. It is shown that the Berthelot-type conduction is dominated in the range 50–150 K. The Berthelot-type conduction mechanism parameters can be affected by annealing temperature, Ni concentration and Ni nanoparticle size. It can be seen that the films annealed at 500℃ have the maximum conductivity. The extents of the carrier wave function at 500℃

have the minima 2.87×10^{-7} cm and 2.45×10^{-7} cm in octahedral-metal stretching vibrations and intrinsic stretching vibrations of the metal at the tetrahedral site, respectively. The average distances between the sites at 500 ℃ also in two vibrations have the minima 1.13×10^{-7} cm and 0.97×10^{-7} cm. It is found that in the Berthelot-type conduction mechanism, the inverse localization parameter α and the average distances between the sites are small. Therefore this study can be used for synthesis of semiconductors that the excitation of carriers to the transport band (high temperatures) and variable range hopping (low temperatures) cannot prevail.

References

[1] Ţălu, Bramowicz M, Kulesza S, Shafiekhani A, Ghaderi A, Mashayekhi F and Solaymani S 2015 *Ind. Eng. Chem. Res.* **54** 8212

[2] Stach S, Garczyk, Ţălu Ş, Solaymani S, Ghaderi A, Moradian R, Nezafat N B, Elahi S M and Gholamali H 2015 *J. Phys. Chem.* C **119** 17887

[3] Naderi S, Ghaderi A, Solaymani S and Golzan M M 2012 *Eur. Phys. J. Appl. Phys.* **58** 20401

[4] ŢăluuS, Stach S, Solaymani S, Moradian R, Ghaderi A, Hantehzadeh M R, Elahi S M, Garczy k and Izadyar S 2015 *J. Electroanal. Chem.* **74** 931

[5] Endrino J L, Galindo R E, Zhang H S, Allen M, Gago R, Espinosa A and Anders A 2008 *Surf. Coat. Technol.* **202** 3675

[6] Ghodselahi T, Vesaghi M A and Shafiekhani A2009 *J. Phys. D: Appl. Phys.* **42** 015308

[7] Ghodselahi T, Vesaghi M A, Shafiekhani A, Ahmadi M, Panahandeh M and HeidariSaani M 2010 *Physica* B **405** 3949

[8] Garcia-Zarco O, Rodil S E and Camacho-Lopez M A 2009 *Thin Solid Films* **518** 1493

[9] Dalouji V, ElahiS M and SaadiAlecasir M 2015 *Phys. Scr.* **90** 115802

[10] Elahi S M, Dalouji V, Mehrparvar D and Valedbagi S 2013 *Mol. Cryst. Liq. Cryst.* **587** 105

[11] Dalouji V and Elahi S M2014 *J. Korean Phys. Soc.* **64** 857

[12] Dalouji V and Elahi S M 2015 *J. Fusion Energy* **34** 646

[13] Islam M N, Ram S K and Kumar S 2009 *Physica* E **41** 1025

[14] Serin T, Yildiz A, andSerinN S H 2011 *Physica* B **406** 3551

[15] Hill R M 1976 *Phys. Status Solidi* A **35** 29

[16] Zabrodski A G and Zinoveva K N 1984 *Sov. Phys. JETP* **59** 425

[17] Tan M, Köseoglu Y, Alan F and Sentürk E 2011 *J. Alloys Compd.* **509** 9399

[18] Ajmal M and Maqsood A 2008 *Mater. Lett.* **62** 2077

[19] Hurd C M 1985 *J. Phys.* C **186** 487

[20] Mehra R M, Agarwal V, Singh V A and Mathur P C 1998 *J. Appl. Phys.* **83** 2235

[21] Singh J and Shimakawa K 2003 *Advances in Amorphous Semiconductors* (Washington: Taylor & Francis)